Science of the Total Environment 914 (2024) 169987

Contents lists available at ScienceDirect

Science of the Total Environment

journal homepage: www.elsevier.com/locate/scitotenv

Multi-season mobile monitoring campaign of on-road air pollution in Bengaluru, India: High-resolution mapping and estimation of quasi-emission factors

Adithi R. Upadhya [a], Meenakshi Kushwaha [a], Pratyush Agrawal [b], Jonathan D. Gingrich [c], Jai Asundi [b], V. Sreekanth [b,*], Julian D. Marshall [d], Joshua S. Apte [e]

[a] ILK Labs, Bengaluru 560046, India
[b] Center for Study of Science, Technology, and Policy, Bengaluru 560094, India
[c] Civil, Architectural, and Environmental Engineering, University of Texas at Austin, TX 51250, United States of America
[d] Civil and Environmental Engineering, University of Washington, Seattle, WA 98195, United States of America
[e] Civil and Environmental Engineering, University of California, Berkeley, CA 94720, United States of America

HIGHLIGHTS

- On-road Black Carbon and Ultrafine Particles were measured in Bengaluru, India.
- Major roads are the most polluted, followed by arterial and residential roads.
- No seasonal patterns in concentrations were observed for on-road air pollution.
- The spatial pattern is similar for quasi-emission factors as for concentrations.

GRAPHICAL ABSTRACT

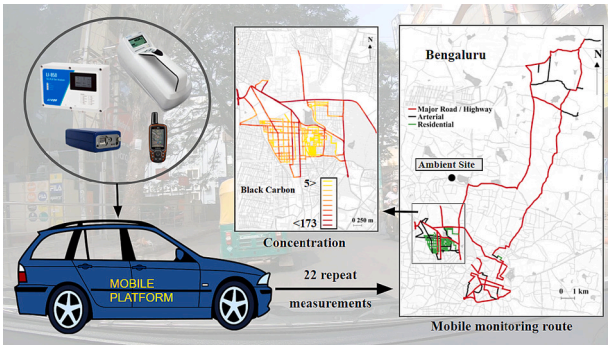

ARTICLE INFO

Editor: Pavlos Kassomenos

Keywords:
Black carbon
CO_2
Monte Carlo subsampling
Quasi-emission factors
Mobile monitoring
Bengaluru, India

ABSTRACT

Mobile monitoring can supplement regulatory measurements, particularly in low-income countries where stationary monitoring is sparse. Here, we report results from a ~ year-long mobile monitoring campaign of on-road concentrations of black carbon (BC), ultrafine particles (UFP), and carbon dioxide (CO_2) in Bengaluru, India. The study route included 150 unique kms (average: ~22 repeat measurements per monitored road segment). After cleaning the data for known instrument artifacts and sensitivities, we generated 30 m high-resolution stable 'data only' spatial maps of BC, UFP, and CO_2 for the study route. For the urban residential areas, the mean BC levels for residential roads, arterials, and highways were ~ 10, 22, and 56 μg m^{-3}, respectively. A similar pattern (highways being characterized by highest pollution levels) was also observed for UFP and CO_2. Using the data from repeat measurements, we carried out a Monte Carlo subsampling analysis to understand the minimum number of repeat measures to generate stable maps of pollution in the city. Leveraging the simultaneous nature of the measurements, we also mapped the quasi-emission factors (QEF) of the pollutants under investigation. The

* Corresponding author.
E-mail address: sree_hcu@yahoo.co.in (V. Sreekanth).

https://doi.org/10.1016/j.scitotenv.2024.169987
Received 8 September 2023; Received in revised form 30 December 2023; Accepted 5 January 2024
Available online 9 January 2024

current study is the first multi-season mobile monitoring exercise conducted in a low or middle -income country (LMIC) urban setting that oversampled the study route and investigated the optimum number of repeat rides required to achieve representative pollution spatial patterns characterized with high precision and low bias. Finally, the results are discussed in the context of technical aspects of the campaign, limitations, and their policy relevance for our study location and for other locations. Given the day-to-day variability in the pollution levels, the presence of dynamic and unorganized sources, and active government pollution mitigation policies, multi-year mobile measurement campaigns would help test the long-term representativeness of the current results.

1. Introduction

Air pollution is one of the leading global risk factors for death and disease (HEI, 2020). Exposure to air pollution and the resulting health effects depend on the microenvironment and the amount of time spent there (Riediker et al., 2004; Jacobs et al., 2010). Traffic-related emissions often constitute an important share of ambient concentrations and personal exposure (HEI, 2010; Guttikunda et al., 2019). While the near-traffic microenvironment has been well characterized in many developed countries (HEI, 2010), on-road air pollution remains understudied in low- and middle-income country (LMIC) settings. Given the dynamic nature of urban pollutants, in many cases, their spatial variations are not well captured by stationary ambient monitors. In that context, mobile monitoring, where in-use sensors are transported in a moving platform (e.g., bicycle, motor vehicle), can be a useful approach to understand and quantify fine-scale spatial variations in pollutant concentrations.

Mobile monitoring studies have been conducted in Europe and North America, with a range of objectives: i) high-resolution mapping of on-road air pollution, ii) exposure assessment, iii) estimation of emission factors, iv) building land-use regression models, and v) understanding the racial and ethnic disparities in pollution level (Birmili et al., 2013; Ruths et al., 2014; Peters et al., 2014; Karjalainen et al., 2014; Patton et al., 2014; Ghassoun et al., 2015; Ježek et al., 2015; Williams and Knibbs, 2016; Apte et al., 2017; Wen et al., 2019; Chambliss et al., 2021; Blanco et al., 2022). Mobile monitoring requires many runs of high resolution, precise measurements. A few studies have reported some best practices for mobile monitoring research in Europe and North America (Van Poppel et al., 2013; Van den Bossche et al., 2015; Alas et al., 2019).

Additional challenges exist when performing mobile monitoring measurements in India. These include: i) poor road conditions resulting in substantial instrument vibration, ii) limited ambient monitors to record background concentrations, and iii) substantial spatiotemporal heterogeneity in pollution levels, sources, and composition. A few studies have attempted to characterize on-road air pollution in India. Apte et al. (2011) reported higher (compared to that of ambient) on-road pollution levels based on ~180 h of mobile monitoring measurements in New Delhi, India. This data was subsequently used to build a land-use regression model for on-road pollution in New Delhi (Saraswat et al., 2013). In a study comparing $PM_{2.5}$ levels for multiple travel modes in New Delhi, Goel et al. (2015) reported that concentrations were lowest in air-conditioned cars and highest while biking. Both et al. (2011) conducted monitoring while walking, to investigate spatial patterns in pollution levels near a roadway, in a low-income and a middle-income neighborhood in Bengaluru. A bicycle-based mobile monitoring campaign of BC and UFP in Bengaluru used spectral noise measurements to successfully predict on-road BC and UFP exposures (Dekoninck et al., 2015). Kolluru et al. (2018) measured commute exposures on 200 km of national highway in Telangana and Andhra Pradesh, India. That study covered six transport modes and reported that traveling by air-conditioned car led to the lowest $PM_{2.5}$ exposure but highest CO exposures. Transport modes explained the highest variability for CO concentrations, followed by CO_2 and $PM_{2.5}$. In an alternative approach in Chennai, researchers used a combination of walking and bus rides along with a customized personal air monitor to map particles and gases in urban road and background settings (Shiva Nagendra et al., 2018). Results from most of the above studies are presented using data from limited repeat measurements without investigation of the minimum requirement for the number of repeat measurements required for establishing stable (representative) pollution maps.

Here, we present results from a ~ year-long mobile monitoring campaign of black carbon (BC), ultrafine particles (UFP), carbon dioxide (CO_2), and meteorological parameters (ambient temperature and relative humidity). Containing 22 drive passes of each route, we use these measurements to: i) generate high-resolution (30 m) on-road air pollution maps at the neighborhood level, ii) investigate the minimum number of repeat measurements required to generate stable pollution maps, and iii) estimate and characterize quasi-emission factors for on-road BC and UFP.

We sought to explore the feasibility of repeated mobile monitoring sampling techniques developed using advanced platforms like Google Street View cars for air quality mapping in an urban setting of LMIC. Urban centers in India generally experience comparatively high levels of pollution, with concentrations often an order of magnitude greater than typical levels in the United States or Europe. Indian cities also feature dynamic and heterogeneous emission sources like waste burning and construction. Flexible air quality mapping using mobile monitoring potentially offers a low-cost solution to fill critical data gaps in regulatory monitoring.

While a few studies in India have explored the utility of mobile monitoring techniques to map on-road air pollution, ours is the first study to investigate the optimum number of repeat samples required to produce stable pollution maps. Our study considers one urban area (Bengaluru, India) and multiple types of urban neighborhoods. To the best of our knowledge, our study is the most comprehensive wall-to-wall mobile monitoring investigation in any LMIC urban center to date, involving a ~ year-long data collection and ~ 150 km of unique roads, covering all major road types. Our measurements facilitate characterizing pollution in many possible urban land use settings.

Our investigation required overcoming some practical challenges associated with mobile monitoring in a LMIC urban center, including poor road infrastructure, densely populated neighborhoods, and frequent gridlocks of traffic. Because we also lacked advanced mobile platforms like Google Street View car and automated navigation, we establish a protocol of adapting the mobile monitoring technique for a similar setting. The results and lessons learned can be used to expand mobile monitoring coverage in similar settings and possibly include other pollutants.

2. Methods

2.1. Study location

We conducted mobile monitoring of air pollution in four regions in Bengaluru, India. The study regions included i) the central business district (CBD), ii) an urban residential area (Malleshwaram, MAL), and iii) a peri-urban area (Kannuru, KAN), and (iv) peri-urban–to-urban transects. Results are given here for the urban residential area (MAL, located in north Bengaluru); results from other areas (CBD; KAN, and the transects) are in the supplementary information. For visual display purposes in this manuscript, the route, data and results for the peri-urban–to-urban transects are combined with KAN; the reason is that the

road length of KAN is smaller and constitutes only arterial roads, and combining with the transects made most sense geographically.

The total road length covered in MAL was ~64 km (out of ~150 km of total road length monitored), comprised of highways (28 %), arterial roads (24 %), and residential roads (48 %). Road classification was obtained from OpenStreetMap (OSM). For the ~10 % of study roads tagged as "unclassified" in OSM, we used visual observations to assign a road type.

Mobile monitoring was conducted from July 10, 2019 until March 12, 2020, covering most of the seasons. Because of the Corona Virus Disease (COVID19) related nationwide lockdown, we were not able to cover the pre-monsoon (March, April, and May) season extensively. Monitoring rides were carried out on (non-rainy) weekdays between 9 am and 1 pm local time (LT). The four-hour window was chosen based on i) endurance of the instruments' batteries, and ii) coverage of morning rush hour peak and afternoon trough in the pollution levels. The MAL study area was divided into two parts (MAL1 and MAL2; Fig. S1), which were covered on different days. The total study route of 150 km (divided into four parts: MAL1, MAL2, CBD, and KAN) as shown in Fig. S2 was covered in the first four weekdays. A few rides (~5) were conducted on Fridays. No daily route was repeated in any week. We made 22 repeat measurements of the total study route (Fig. S3).

2.2. Instrumentation

2.2.1. Mobile platform

During the campaign, we measured on-road BC, UFP, CO_2, ambient temperature, and relative humidity (RH), along with the Global Positioning System (GPS) location. All air pollution monitoring instruments were mounted on a mobile platform, which is a compressed natural gas (CNG)-powered hatchback passenger car (Maruti Suzuki Celerio). A CNG car was preferred due to its low tailpipe emissions (to reduce self-pollution) compared to petrol and diesel cars. Instruments were placed near the rear window with the inlets of the instruments near to the open window. To reduce road vibration, instruments were cushioned and strapped with bungee cords. All instruments used on the mobile platform were portable, battery-operated, factory-calibrated, and set to measure and data-log at one-second (1 Hz) temporal resolution. (As described below, one instrument, the rack-mounted aethalometer, was fixed-site rather than mobile.)

2.2.2. Location

A GPS receiver (Garmin GPSMAP 64 s) and a smartphone-based application were used to collect the latitude and longitude information of the mobile vehicle. All instruments' times were synchronized to the GPS time daily prior to monitoring.

2.2.3. Black carbon (BC)

A microAeth (AE51, AethLabs, San Francisco, USA) was used to measure the real-time on-road black carbon mass concentration. AE51 is a filter-based pocket-size instrument that works on the aethalometer optical absorption principle (Hansen et al., 1984). In AE51, the change in the rate of optical absorption (at 880 nm) by the particle sample is converted into BC using a factory-supplied mass absorption efficiency value. The measurement range of AE51 is 0 to 1 mg m^{-3}. During the measurement campaign, AE51 was operated at a flow rate of 100 mL min^{-1}. For each ride, a new filter ticket was used.

2.2.4. Ultrafine particle number concentration (UFP)

A handheld Condensation Particle Counter (Model 3007, TSI Incorporated, Minnesota, USA) was used to measure the on-road particle number concentration. The detection size range of the instrument is 10 nm to >1 μm. Because the particle number size distribution is dominated by particles smaller than 100 nm, we use this measurement of particle number count as a measure of the ultrafine particle (UFP) number concentration. The instrument uses isopropanol as its working fluid (condensate), which condenses on the aerosol particles and increases the particle size such that they can be detected and counted optically. The flow rate is 0.7 L min^{-1}. Before each ride, zero-check was performed to detect contamination of the optics. The manufacturer-defined instrument measurement range is 0 to 100,000 particles cm^{-3}. (For concentrations above the manufacturer-defined maximum, the instrument operates and reports concentrations, but readings are increasingly under-counts owing to coincident counting.) As the on-road particle concentration in Bengaluru exceeded the manufacturer-defined measurement range, we operated the CPC3007 along with a diluter (with a dilution ratio ~ 5.5). The dilution ratio was validated by operating the CPC3007 sequentially with and without the diluter (repeatedly, 5 min in each configuration) in a closed and concentration-stable room. The design of the diluter is described in Ban-Weiss et al. (2009) and Apte et al. (2011). A study by Jørgensen (2019) has shown variability in the CPC3007 measurements when compared to the UFP measurements made by Scanning Mobility Particle Sample (SMPS), which could be largely because of differences in the cut-off size, i.e., the smallest particle detectable by an instrument.

2.2.5. Carbon dioxide (CO_2)

To measure on-road CO_2 concentrations, we used a LI-850 analyzer (Li-COR, Inc., Lincoln, USA), which employs the non-dispersive infrared (NDIR) absorption technique. Its measurement range is 0 to 20,000 ppm with an accuracy of 1.5 %. The lower limit of detection for the instrument is 1.5 ppm and the nominal flow rate of the instrument is 0.75 L min^{-1}.

2.2.6. Temperature and RH

An RH probe (RH-USB, Omega Engineering Inc., Connecticut, US) was used to measure temperature and RH. The device measurement range is 2 % to 98 % for RH and − 17 to 49 °C for temperature.

2.2.7. Ambient BC

A rack-mount seven-channel aethalometer (AE33, Magee Scientific, Berkeley, USA) was used to measure the ambient BC at one-minute averaging intervals at a fixed site. AE33 is a filter tape-based instrument that works on the light-absorption principle, similar to that of AE51 (Hansen et al., 1984). AE33 is a dual spot aethalometer that measures absorption in seven channels with an inbuilt loading correction algorithm; absorption at 880 nm was considered as BC. AE33 is also capable of distinguishing between fossil fuel burning and biomass burning-emitted BC. During the study period, AE33 was operated at 2 L min^{-1} with a 2.5 μm size cut cyclone installed to the sample inlet. The instrument was installed inside at the Center for Study of Science, Technology, and Policy (CSTEP, located in north Bengaluru) aerosol laboratory (~5 m above ground level), with the inlet tubing protruding outside (ambient air). CSTEP is ~110 m away from a major road.

2.3. Data analysis

All analysis presented in this manuscript was performed using the open source 'R' programming language (www.r-project.org).

2.3.1. On-road BC

BC data required rigorous cleaning and quality check due to the sensitivity of AE51 to vibration and shock, which, owing to the poor road conditions, was common during the rides, even as cushioning was used to dampen vibrations. We used the algorithm developed and described by Apte et al. (2011) for identifying spurious values attributable to the vibration effect. The algorithm identified ~9 % of the one-second BC data as spurious and removed those from further analysis. Next, the correction equation developed by Kirchstetter and Novakov (2007) was applied to the BC data to account for the well-understood loading effect in BC measurements by filter-based equipment. AE51's underestimates of BC concentrations increase as the particle sample

accumulates on the filter ticket. The loading correction equations are.

$$BC = BC_{raw}{}^{*} (0.88^{*} Tr + 0.12)^{-1} \quad (1)$$

$$Tr = exp(-ATN/100) \quad (2)$$

where *Tr* is the filter transmission, and BC_{raw} and *ATN* are the instrument's reported concentration and attenuation values, respectively. For all references hereafter, *BC* is the loading-corrected BC mass concentration.

2.3.2. UFP

As the condensation particle counter operated along with a diluter, raw UFP values were multiplied by the dilution ratio (*DR*) to obtain the real concentrations.

$$UFP = UFP_{raw}{}^{*} DR \quad (3)$$

For all references hereafter, *UFP* is dilution-corrected particle number concentration.

2.3.3. CO_2

For CO_2 measurements, we are interested in concentrations relative to background levels, a metric we term ΔCO_2. Therefore, CO_2 measurements were adjusted by subtracting the ride (daily) minimum value from each of the one-second values measured in that particular ride:

$$\Delta CO_2 = CO_{2-raw} - CO_{2\ daily\ minimum} \quad (4)$$

2.3.4. Snapping and gridding

After cleaning and correcting the pollutant concentration data, we added location information from GPS. Each location (latitude and longitude) is snapped to the nearest OSM road, thereby allowing statistical analysis of repeated measurements at the same location despite subtle differences in GPS tracks between repeated drive passes. Following the approach of Messier et al. (2018), the entire route was divided into 30 m road segments, and the concentration data were assigned to the corresponding (i.e., nearest) 30 m segment. Daily, the mean concentration per segment was computed for each of the pollutants for the entire study region. To generate the study period aggregate map of each pollutant, the median of the daily means was used, as in Messier et al. (2018).

2.3.5. Bootstrap resampling

We used bootstrap resampling to understand robustness in the choice of the central tendency statistic used in the study. Using the one-second measurements in a particular 30 m road segment and resampled data (10,000 times with replacement), we computed the central tendency statistics (mean and median). We observed that the standard error of the median computed from the observations and the standard deviation of the median for the bootstrapped subsamples were almost equal for all the road segments.

2.3.6. Intraclass correlation (ICC)

We computed intraclass correlation, a metric of the reliability of repeated measures that varies between 0 and 1, by binning the pollution data based on road types, to investigate the robustness in the pollutant spatial variations. ICC is the ratio of variability between different groups (road segments) to the variability within groups (measurements for each road segment). A high value of ICC (> 0.75) indicates that variability is more prominent between groups than within groups.

2.3.7. Monte Carlo analysis

We performed a Monte Carlo subsampling analysis to investigate if the air pollution data collected from a lesser number of rides can produce stable maps or not. This analysis sheds light on the point of "diminishing returns" (in terms of the number of rides), beyond which, adding more data would not appreciably change the pollution maps. Here, we subsampled (without replacement) the daily mean pollutant value for each road segment. For $N = 2, 4, 6, 8, 10, 12, 14, 16$, and 18, we performed 100 random draws, hence producing 100 subsampled median maps (for each N ride). For road segments having measurements less than N, all the data was included to create a subsampled median map. As N increases, the subsampled data tends to be similar to the total number of rides. Data from each subsampled map was then compared with the concentration median maps derived from the full dataset ($N = 22$ rides). The coefficient of determination (R^2, a metric of precision) and normalized root mean square error (NRMSE, a metric of accuracy) was computed for each comparison.

2.3.8. Quasi-emission factors

Because our data include simultaneous measurements of pollutants (BC, UFP) and CO_2, we are able to derive real-time on-road quasi-emission factors (QEFs). QEF is the real-time ratio of the pollutant concentration (BC or UFP) to ΔCO_2. (As described above, ΔCO_2 refers to background-subtracted CO_2, i.e., representing the real-time on-road increment in CO_2.) The "quasi" in "QEF" reflects that (1) to convert the QEF to an actual emission factor requires assumptions regarding the chemical composition of the fuel (e.g., for octane [C_8H_{18}], complete combustion of each molecule of fuel would generate 8 molecules of CO_2), and (2) a small portion of the fuel will incompletely combust, thereby forming CO, BC, or other organic emissions instead of CO_2; a more-complete estimate for emission factors would incorporate CO measurements. Nevertheless, the QEF provides a useful proxy for emission factors (grams emitted per liter of fuel consumed), and how they vary in time, space, and with respect to specific attributes (e.g., road-type, traffic speed).

3. Results

3.1. Spatial variations

Around 300,000 1-Hz concentration measurements (~83 h) of each pollutant were made in the urban residential neighborhood of Malleshwaram (MAL). The number of data points collected reflects in part the speed of the vehicle—the slower the vehicle, the higher the number of measurements per road segment. The average speed of the mobile monitoring vehicle in MAL was ~13 km h^{-1}. MAL is comprised of 2142 road segments (30 m each; total monitored road length in MAL: 64 km; see Table S1). Fig. 1 shows spatial variation of on-road BC, UFP, and ΔCO_2 (median of daily mean concentrations, for each 30 m road segment) in MAL. The spatial mean (median) for MAL is ~26 μg m^{-3} (15 μg m^{-3}) BC, ~81,000 # cm^{-3} (62,000 # cm^{-3}) UFP, and 49 ppm (42 ppm) ΔCO_2.

The gridded spatial variations in the pollutant concentrations for other study regions (CBD and KAN) are in Figs. S4 and S5. For the combined peri-urban, peri-urban–urban transects, the number of road segments was 2108, and the spatial mean (median) concentrations are ~39 μg m^{-3} (34 μg m^{-3}) BC, 82,000 # cm^{-3} (79,000 # cm^{-3}) UFP, and 53 ppm (49 ppm) CO_2. The central business district (CBD) is comprised of 740 road segments; spatial mean (median) concentrations were ~ 46 μg m^{-3} (41 μg m^{-3}) BC, 143,000 # cm^{-3} (139,000 # cm^{-3}) UFP, and 92 ppm (83 ppm) CO_2. For all three pollutants, the most polluted road segments are the highways, followed by arterials and residential (Fig. 2; Tables S2-S4). The differences in the pollutant concentrations by road type were statistically significant based on a one-way ANOVA ($p < 0.001$) test.

We computed intra-class correlation (ICC) values for the 30 m road segments as a measure of the temporal stability of subsampled spatial patterns (Tables S5 to S7). ICC values of all parameters for MAL ranged between 0.81 and 0.92, indicating systematic spatial differences (between road segments) and comparatively little residual variability within each road segment. ICC values for KAN ranged between 0.69 and

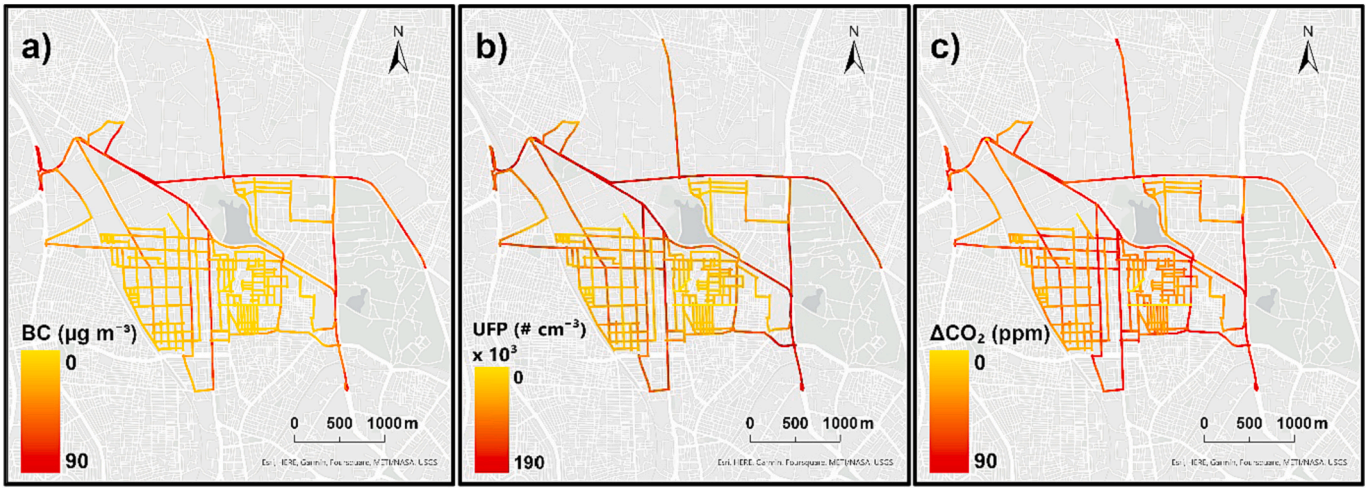

Fig. 1. Spatial maps of on-road a) BC, b) UFP, and c) ΔCO_2. BC = black carbon; UFP = Ultrafine Particle number concentration; ΔCO_2 = delta carbon dioxide, i.e., the measured on-road CO_2 concentration minus the background CO_2 concentration.

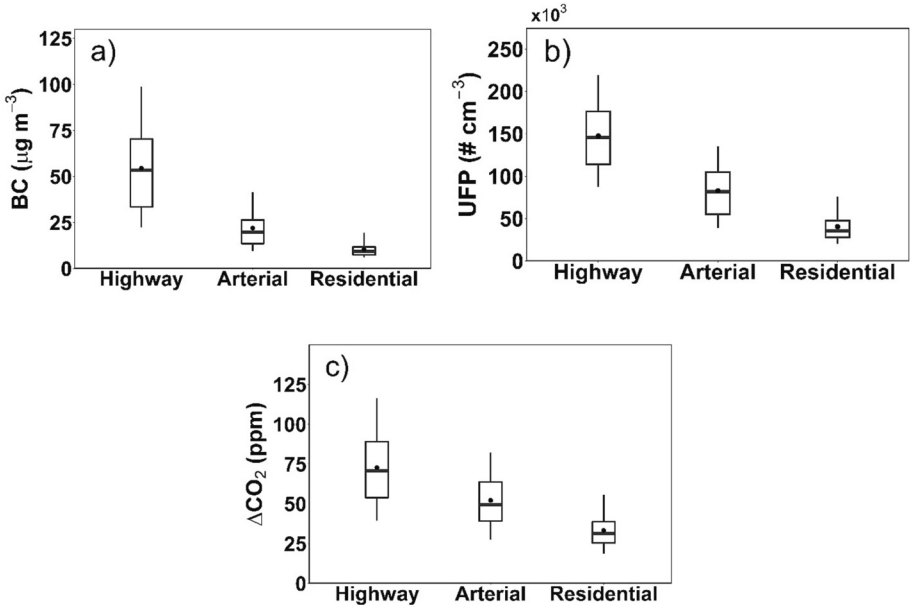

Fig. 2. Pollutant concentration distribution by road type for the median of drive pass-means, for a) BC, b) UFP, and c) ΔCO_2. The whiskers represent the 5th and 95th percentile, the box represents the 25th and 75th percentile, and the median and mean are shown by the line and point inside the box, respectively.

0.94, and for CBD, between 0.72 and 0.86. A closer look at road types revealed the lowest ICC values on arterial (0.43 for CO_2) and residential roads (0.43 for BC and 0.54 for UFP) in KAN.

The BC versus UFP hex plot (Fig. S6) shows variability in the pollutant concentrations (median of daily drive-pass means). At lower values of BC and UFP, the data followed a linear relation. Beyond 150,000 # cm^{-3}, UFP seem to be relatively constant even with BC increases further. As described above, we used a dilutor with a factor of ~5.5 dilution; thus, this saturation effect in the range 150,000 to 300,000 (i.e., for which the instrument reads 27,000 to 54,000) is not attributable to measurements exceeding the manufacturer-defined concentration range. The adjusted R^2 for the fit is 0.30 for highways, 0.25 for arterials, and 0.55 for residential roads.

3.2. Monte Carlo analysis

Results from the Monte Carlo subsampling analysis for BC and UFP (Fig. 3) for MAL reveal that the gain in R^2 with the inclusion of each additional ride data increased rapidly until about 7 sampling days (for both BC and UFP) and slowly thereafter. At ~10 sampling days, R^2 is close to 0.8. Similarly, normalized root mean square error (NRMSE) curves (Fig. 3b and d) show that the error rapidly decreased with the inclusion of each additional sampling day, with a sharp decrease in slope after day 6. Unlike R^2, NRMSE values continuously decreased without leveling off. If we pool data from all study routes for Monte Carlo subsampling (Fig. S7), there is no clear "point of diminishing return", and at least 10 repeat measurements are required to achieve $R^2 > 0.75$. Figs. S8 and S9 show the Monte Carlo analysis by road type. Results for BC and UFP by road types are similar to that observed for MAL. The "point of diminishing return" is observed to be similar among road types, although the error (NRMSE) differed by ~20 % across the road types.

3.3. Quasi-emission factors (QEF)

The spatial pattern of QEFs (Fig. 4, Tables S8, S9 and S10) mostly followed the pollutant spatial pattern. The higher QEFs on highways

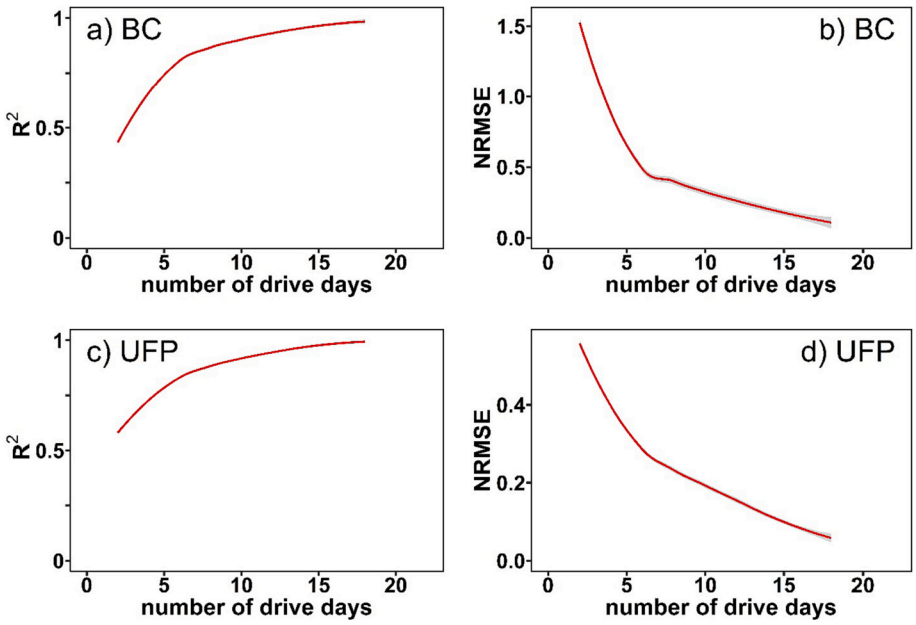

Fig. 3. Monte-Carlo subsampling analysis for the MAL neighborhood, showing R^2 values (left column), and normalized root-mean-square-error (right column). Panels a) and b) correspond to BC, c) and d) correspond to UFP.

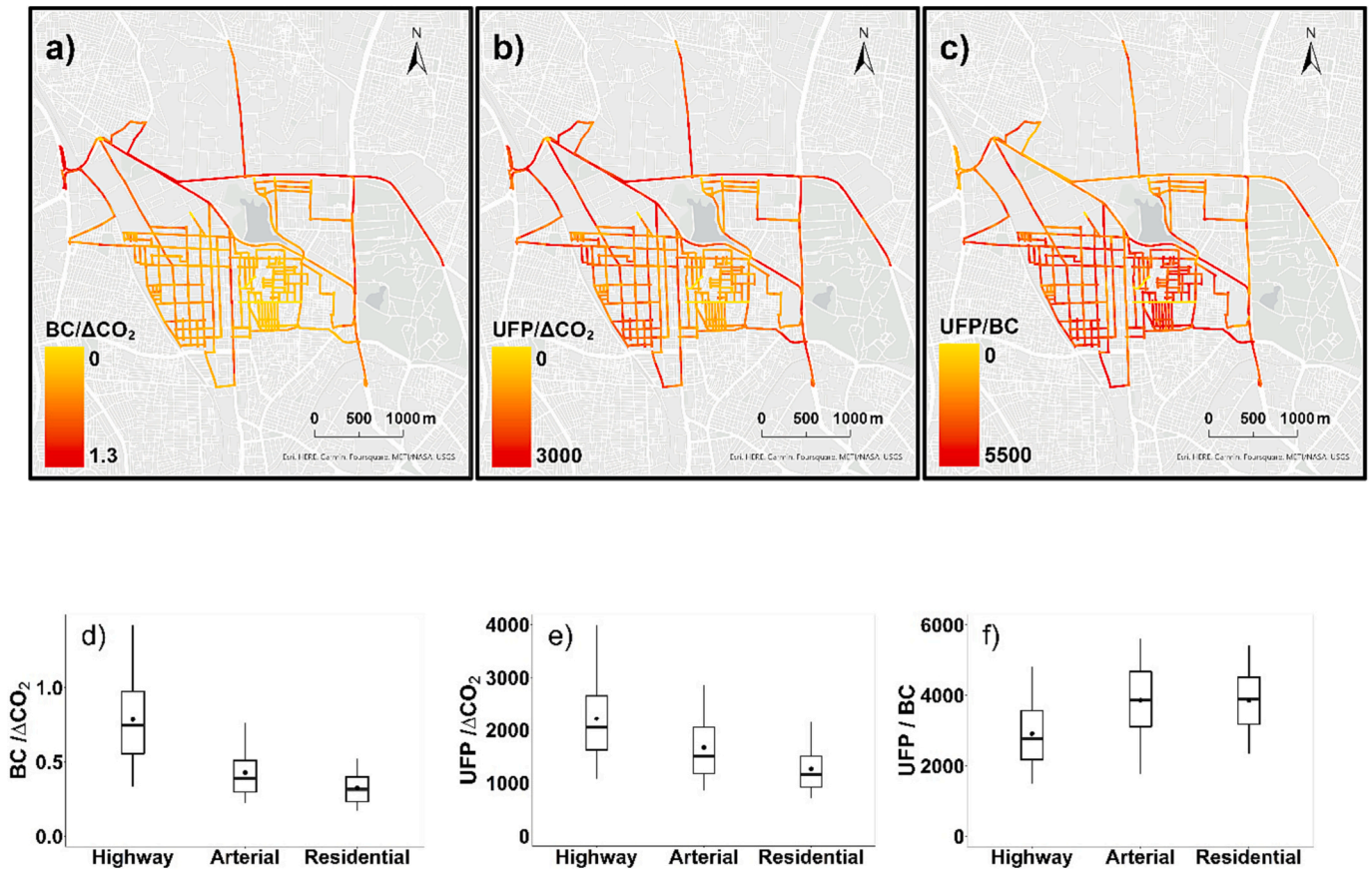

Fig. 4. Gridded spatial variation and box plots of $BC/\Delta CO_2$ (BC QEF), $UFP/\Delta CO_2$ (UFP QEF), and UFP/BC. The whiskers represent the 5th and 95th percentile, the box edges represent the 25th and 75th percentile, and the median and mean are shown by the line and point inside the box respectively.

may be attributable to heavy-duty diesel vehicles, whose particulate emission factors can be much higher than that of light motor vehicles, which are mostly petrol and CNG operated. The mean values for QEFs (Table S8) indicate that BC emissions per liter of fuel are ~2 times higher on highways than on arterial roads, and ~ 20–70 % less on residential roads than on arterial roads. For UFP, QEFs relative to arterials were ~ 20–85 % higher on highways and ~ 8–20 % lower on (except KAN) residential roads (Table S9). QEFs (and pollutant levels) increased

with increases in the traffic speed is observed for all the road types and pollutants (Fig. S10).

3.4. Ambient and on-road BC

Median concentrations were 2.9 μg m^{-3} (November) to 6.2 μg m^{-3} (August) for ambient conditions (CSTEP fixed site) and 9.7 μg m^{-3} (December) to 19.9 (October) μg m^{-3} for on-road conditions (Fig. S11). On average, on-road BC values are nearly ten times higher than that of the ambient. Seasonal patterns are substantially greater for ambient BC than for on-road BC. For example, the ratio of BC concentrations in September versus in December is ~1.8 for ambient, ~1.2 for on-road.

4. Discussion

The present study is one of the few large-scale repeated mobile monitoring exercises conducted in India. We made a total of 22 repeat measurements over the study route to construct high-resolution, neighborhood-level, stable, on-road pollution maps. We followed best practices (related to instrument maintenance and data analysis) in conducting a mobile monitoring campaign of air pollutants, as outlined in Alas et al. (2019). Results here shed light on adaptability of mobile monitoring technique in a middle-income-country urban setting with relative higher pollution levels.

Our study revealed large spatial variability in pollutant concentrations within the residential neighborhood and also by road type (Figs. 1 and 2) in Bengaluru. The difference in pollution levels between road types is more pronounced for BC than for CO_2 and UFP. Highways experienced average BC concentrations of about five times that of residential roads and at least twice that of arterial roads (Table S2). Even within the same road type, variability in pollutants concentrations between road segments was observed. The ICC values for all parameters in MAL ranged between 0.81 and 0.95, indicating a significant difference in pollution levels between road types. On-road CO_2 followed the same pattern as BC and UFP, suggesting that spatial variation in on-road pollution is likely due to the differences in on-road traffic volumes. Ambient concentrations are nearly 10 times lower than on-road concentrations (Fig. S9), further demonstrating large spatial differences in exposure and ambient pollution levels.

Measurements of on-road UFP concentrations are scarce in India. For comparison, the mean on-road UFP concentration in Bengaluru (current study) coincided with the lower end of measurements from a mobile monitoring study in New Delhi, a city with historically higher background levels of pollution (Apte et al., 2011). Average BC concentrations reported from measurements carried over 60 round trips during early spring and summer in an autorickshaw in New Delhi were about twice that observed in this study. In contrast, mean estimates of on-road BC and UFP in the current study were twice that of stationary measurements at LUR sites in Delhi (Saraswat et al., 2013). Notably, both the studies referenced here (i.e., by Apte et al. and by Saraswat et al.) reported geometric means, unlike the arithmetic mean reported in our study.

To test the generalizability of the results obtained from MAL, we investigated the data collected in other parts of the city with distinctly different characteristics (Figs. S4 and S5). Overall, we observed that all pollutant concentrations had the lowest values in urban and peri-urban residential neighborhoods. The urban-to-rural pollution gradient (Fig. S5) involves highest on-road concentrations in the urban area, decreasing through the urban–peri-urban transect and the lowest levels in the peri-urban area. The overall highest concentrations were in the urban business district. For all three neighborhoods (MAL, CBD, KAN), CO_2 maps mirrored the UFP and BC maps.

As described above (Section 3.3), after ~10 rides, each additional ride-day does not contribute as much to improving precision. One cannot identify a single, precise "point of diminishing returns" (i.e., the curves in Fig. 3 do not fully asymptote, nor do they have a specific, consistent inflection point). If future research aims to more-robustly identify the "point of diminishing returns" (i.e., to have the curves in Fig. 3 asymptote), it likely would be beneficial to conduct more visits per location. When we pool data from the entire study (i.e., CBD, KAN, and MAL; see Fig. S7), this point is not reached within the number of drive-days we have conducted. This result might be due to larger day-to-day variations in pollutant concentrations. CBD and KAN are characterized by more highway road segments, so we would expect greater temporal heterogeneity in the traffic type, volumes, and speed, relative to MAL. Therefore, to generate a stable pollution map in these areas, a larger number of rides (relative to Fig. 3 / just for MAL) are required. The results from MAL (Fig. 3) are encouraging though, and in agreement with that obtained in urban Oakland (Apte et al., 2017). With weekday sampling, they found that for BC and NO, at least ~10 rides were required to achieve the "point of diminishing return".

Mobile monitoring is being adapted in multiple cities to complement the regulatory monitoring data (e.g., Breathe London Project, 2018). However, this technique remains under-utilized in LMICs. While some studies in India have used mobile platforms to measure pollutants in different on-road microenvironments, they are either limited in spatial/temporal coverage or focused on commute exposures. The current study systematically investigated the minimum requirements to generate stable high-resolution pollution maps. Results obtained and lessons learned from this study can be exploited in expanding the mobile monitoring coverage, and also, in working to include other pollutant measurements (gaseous pollutants). Our results (irrespective of road type), showing that a smaller number of rides (~10 rides for the MAL neighborhood) can achieve stable maps (with ~80 % precision), are an encouraging observation in terms of prospects of this technique in Indian, and potentially other, urban settings. In contrast, in a study performed in Mol city (Belgium) by Van den Bossche et al. (2015), the minimum number of rides required to arrive at the representative average pollution concentration varied by road type. The number of stationary monitors in India is increasing slowly, in part because of the high cost of acquiring and maintaining regulatory stations. A recent air pollution quantification framework for India proposed an integrated approach, including with intermittent use of mobile monitoring to capture high-resolution spatial and temporal data (Brauer et al., 2019). In keeping with that framework, the current study demonstrates the feasibility of conducting a mid-cost mobile monitoring infrastructure in low- and middle-income countries.

We found (Section 3.4) that quasi-emission factors for BC and UFP were highest on highways. This finding likely reflects the higher proportion of heavy-duty diesel vehicles on highways compared to residential and arterial roads. Mobile monitoring data has been used to compute vehicle-based emission factors (Larson et al., 2017). In a 5-day mobile monitoring campaign-based study in Chengdu, China, Wen et al. (2019) used absolute principal component analysis to tease out polluting heavy-duty diesel vehicles on highways based on the emission factors. Notably, the emission factors estimated using mobile monitoring air pollution data can be highly sensitive to the emissions from high-emitter vehicles (Kelp et al., 2020).

Our study has a few limitations and challenges. They include: i) measurements were limited to daytime and weekdays, ii) the mobile platform is a CNG car, which is relatively low-emitting but not completely emissions-free. The choice of the vehicle was based on the distance to be covered during the rides; we were unable to find locally a realistic zero-emissions (i.e., electric) car with the required range. iii) Unplanned and indefinite road closures led to occasional changes of the study route and necessitated manual navigation. iv) Results presented here correspond to non-criteria pollutants; monitoring of criteria pollutants could be of greater interest to policymakers.

CRediT authorship contribution statement

Adithi R. Upadhya: Formal analysis, Visualization, Writing –

original draft. **Meenakshi Kushwaha:** Formal analysis, Funding acquisition, Project administration, Validation, Writing – original draft. **Pratyush Agrawal:** Investigation. **Jonathan D. Gingrich:** Investigation. **Jai Asundi:** Funding acquisition, Project administration, Resources, Writing – review & editing. **V. Sreekanth:** Funding acquisition, Investigation, Writing – review & editing. **Julian D. Marshall:** Conceptualization, Funding acquisition, Methodology, Resources, Supervision, Writing – review & editing. **Joshua S. Apte:** Conceptualization, Funding acquisition, Methodology, Resources, Supervision, Writing – review & editing.

Declaration of competing interest

The authors declare that they have no known competing financial interests or personal relationships that could have appeared to influence the work reported in this paper.

Data availability

Data will be made available on request.

Acknowledgments

VS and JA are grateful to MacArthur Foundation and Google for providing financial support to CSTEP for conducting air pollution studies in Bengaluru. Work by JSA and JG was supported by the Health Effects Institute, an organization jointly funded by the US EPA (Assistance Award No. R-82811201) and certain motor vehicle and engine manufacturers. The views expressed in this document are solely those of authors and do not necessarily reflect the views of HEI, or its sponsors, nor do they necessarily reflect the views and policies of the EPA or motor vehicle and engine manufacturers. EPA does not endorse any products or commercial services mentioned in this publication.

Appendix A. Supplementary data

Supplementary data to this article can be found online at https://doi.org/10.1016/j.scitotenv.2024.169987.

References

Alas, H.D.C., Weinhold, K., Costabile, F., Ianni, A.D., Müller, T., Pfeifer, S., Liberto, L.D., Turner, J.R., Wiedensohler, A., 2019. Methodology for high-quality mobile measurement with focus on black carbon and particle mass concentrations. Atmos. Meas. Tech. 12 (9), 4697–4712. https://doi.org/10.5194/amt-12-4697-2019.

Apte, J.S., Kirchstetter, T.W., Reich, A.H., Deshpande, S.J., Kaushik, G., Chel, A., Marshall, J.D., Nazaroff, W.W., 2011. Concentrations of fine, ultrafine, and black carbon particles in auto-rickshaws in New Delhi. India. Atmos. Environ. 45 (26), 4470–4480. https://doi.org/10.1016/j.atmosenv.2011.05.028.

Apte, J.S., Messier, K.P., Gani, S., Brauer, M., Kirchstetter, T.W., Lunden, M.M., Marshall, J.D., Portier, C.J., Vermeulen, R.C., Hamburg, S.P., 2017. High-resolution air pollution mapping with Google street view cars: exploiting big data. Environ. Sci. Technol. 51 (12), 6999–7008. https://doi.org/10.1021/acs.est.7b00891.

Ban-Weiss, G.A., Lunden, M.M., Kirchstetter, T.W., Harley, R.A., 2009. Measurement of black carbon and particle number emission factors from individual heavy-duty trucks. Environ. Sci. Technol. 43 (5), 1419–1424. https://doi.org/10.1021/es8021039.

Birmili, W., Rehn, J., Vogel, A., Boehlke, C., Weber, K., Rasch, F., 2013. Micro-scale variability of urban particle number and mass concentrations in Leipzig. Germany. Meteorol. Z. 22, 155–165. https://doi.org/10.1127/0941-2948/2013/0394.

Blanco, M.N., Gassett, A., Gould, T., Doubleday, A., Slager, D.L., Austin, E., Seto, E., Larson, T.V., Marshall, J.D., Sheppard, L., 2022. Characterization of annual average traffic-related air pollution concentrations in the greater Seattle area from a year-long Mobile monitoring campaign. Environ. Sci. Technol. 56 (16), 11460–11472. https://doi.org/10.1021/acs.est.2c01077.

Both, A.F., Balakrishnan, A., Joseph, B., Marshall, J.D., 2011. Spatiotemporal aspects of real-time $PM_{2.5}$: low-and middle-income neighborhoods in Bangalore, India. Environ. Sci. Technol. 45 (13), 5629–5636. https://doi.org/10.1021/es104331w.

Brauer, M., Guttikunda, S.K., Nishad, K.A., Dey, S., Tripathi, S.N., Weagle, C., Martin, R. V., 2019. Examination of monitoring approaches for ambient air pollution: a case study for India. Atmos. Environ. 216, 116940 https://doi.org/10.1016/j.atmosenv.2019.116940.

Breathe London Project, 2018. Accessed 5th January, 2023. https://www.breathelondon.org/.

Chambliss, S.E., Pinon, C.P., Messier, K.P., LaFranchi, B., Upperman, C.R., Lunden, M.M., Robinson, A.L., Marshall, J.D., Apte, J.S., 2021. Local-and regional-scale racial and ethnic disparities in air pollution determined by long-term mobile monitoring. Proc. Natl. Acad. Sci. 118 (37), e2109249118 https://doi.org/10.1073/pnas.2109249118.

Dekoninck, L., Botteldooren, D., Panis, L.I., Hankey, S., Jain, G., Karthik, S., Marshall, J., 2015. Applicability of a noise-based model to estimate in-traffic exposure to black carbon and particle number concentrations in different cultures. Environ. Int. 74, 89–98. https://doi.org/10.1016/j.envint.2014.10.002.

Ghassoun, Y., Ruths, M., Löwner, M.O., Weber, S., 2015. Intra-urban variation of ultrafine particles as evaluated by process related land use and pollutant driven regression modelling. Sci. Total Environ. 536, 150–160. https://doi.org/10.1016/j.scitotenv.2015.07.051.

Goel, R., Gani, S., Guttikunda, S.K., Wilson, D., Tiwari, G., 2015. On-road PM2. 5 pollution exposure in multiple transport microenvironments in Delhi. Atmos. Environ. 123, 129–138. https://doi.org/10.1016/j.atmosenv.2015.10.037.

Guttikunda, S.K., Nishadh, K.A., Gota, S., Singh, P., Chanda, A., Jawahar, P., Asundi, J., 2019. Air quality, emissions, and source contributions analysis for the Greater Bengaluru region of India. Atmos. Pollut. Res. 10 (3), 941–953. https://doi.org/10.1016/j.apr.2019.01.002.

Hansen, A.D.A., Rosen, H., Novakov, T., 1984. The aethalometer—an instrument for the real-time measurement of optical absorption by aerosol particles. Sci. Total Environ. 36, 191–196. https://doi.org/10.1016/0048-9697(84)90265-1.

HEI, 2010. Panel on the Health Effects of Traffic-Related Air Pollution. Traffic-Related Air Pollution: A Critical Review of the Literature on Emissions, Exposure, and Health Effects.

HEI, 2020. State of Global Air 2020. Special Report.. Health Effects Institute, Boston, MA.

Jacobs, L., Nawrot, T.S., De Geus, B., Meeusen, R., Degraeuwe, B., Bernard, A., Sughis, M., Nemery, B., Panis, L.I., 2010. Subclinical responses in healthy cyclists briefly exposed to traffic-related air pollution: an intervention study. Environ. Health 9 (1), 1–8. https://doi.org/10.1186/1476-069X-9-64.

Ježek, I., Katrašnik, T., Westerdahl, D., Močnik, G., 2015. Black carbon, particle number concentration and nitrogen oxide emission factors of random in-use vehicles measured with the on-road chasing method. Atmos. Chem. Phys. 15 (19), 11011–11026. https://doi.org/10.5194/acp-15-11011-2015.

Jørgensen, R.B., 2019. Comparison of four nanoparticle monitoring instruments relevant for occupational hygiene applications. J. Occup. Med. Toxicol. 14 (1), 1–14. https://doi.org/10.1186/s12995-019-0247-8.

Karjalainen, P., Pirjola, L., Heikkilä, J., Lähde, T., Tzamkiozis, T., Ntziachristos, L., Keskinen, J., Rönkkö, T., 2014. Exhaust particles of modern gasoline vehicles: a laboratory and an on-road study. Atmos. Environ. 97, 262–270. https://doi.org/10.1016/j.atmosenv.2014.08.025.

Kelp, M., Gould, T., Austin, E., Marshall, J.D., Yost, M., Simpson, C., Larson, T., 2020. Sensitivity analysis of area-wide, mobile source emission factors to high-emitter vehicles in Los Angeles. Atmos. Environ. 223, 117212 https://doi.org/10.1016/j.atmosenv.2019.117212.

Kirchstetter, T.W., Novakov, T., 2007. Controlled generation of black carbon particles from a diffusion flame and applications in evaluating black carbon measurement methods. Atmos. Environ. 41 (9), 1874–1888. https://doi.org/10.1016/j.atmosenv.2006.10.067.

Kolluru, S.S.R., Patra, A.K., Sahu, S.P., 2018. A comparison of personal exposure to air pollutants in different travel modes on national highways in India. Sci. Total Environ. 619, 155–164. https://doi.org/10.1016/j.scitotenv.2017.11.086.

Larson, T., Gould, T., Riley, E.A., Austin, E., Fintzi, J., Sheppard, L., et al., 2017. Ambient air quality measurements from a continuously moving mobile platform: estimation of area-wide, fuel-based, mobile source emission factors using absolute principal component scores. Atmos. Environ. 152, 201–211. https://doi.org/10.1016/j.atmosenv.2016.12.037.

Messier, K.P., Chambliss, S.E., Gani, S., Alvarez, R., Brauer, M., Choi, J.J., Hamburg, S.P., Kerckhoffs, J., LaFranchi, B., Lunden, M.M., Marshall, J.D., 2018. Mapping air pollution with Google Street View cars: efficient approaches with mobile monitoring and land use regression. Environ. Sci. Technol. 52 (21), 12563–12572. https://doi.org/10.1021/acs.est.8b03395.

Patton, A.P., Perkins, J., Zamore, W., Levy, J.I., Brugge, D., Durant, J.L., 2014. Spatial and temporal differences in traffic-related air pollution in three urban neighborhoods near an interstate highway. Atmos. Environ. 99, 309–321. https://doi.org/10.1016/j.atmosenv.2014.09.072.

Peters, J., Van den Bossche, J., Reggente, M., Van Poppel, M., De Baets, B., Theunis, J., 2014. Cyclist exposure to UFP and BC on urban routes in Antwerp, Belgium. Atmos. Environ. 92, 31–43. https://doi.org/10.1016/j.atmosenv.2014.03.039.

Riediker, M., Cascio, W.E., Griggs, T.R., Herbst, M.C., Bromberg, P.A., Neas, L., Williams, R.W., Devlin, R.B., 2004. Particulate matter exposure in cars is associated with cardiovascular effects in healthy young men. Am. J. Respir. Crit. Care Med. 169 (8), 934–940. https://doi.org/10.1164/rccm.200310-1463OC.

Ruths, M., von Bismarck-Osten, C., Weber, S., 2014. Measuring and modelling the local-scale spatio-temporal variation of urban particle number size distributions and black carbon. Atmos. Environ. 96, 37–49. https://doi.org/10.1016/j.atmosenv.2014.07.020.

Saraswat, A., Apte, J.S., Kandlikar, M., Brauer, M., Henderson, S.B., Marshall, J.D., 2013. Spatiotemporal land use regression models of fine, ultrafine, and black carbon particulate matter in New Delhi. India. Environ. Sci. Technol. 47 (22), 12903–12911. https://pubs.acs.org/doi/abs/10.1021/es401489h.

Shiva Nagendra, S.M., S.N., Yasa, P.R., Narayana, M.V., Khadirnaikar, S., Rani, P., 2018. Mobile monitoring of air pollution using low cost sensors to visualize spatio-

temporal variation of pollutants at urban hotspots. Sustain. Cities Soc. 44, 520–535. https://doi.org/10.1016/j.scs.2018.10.006.

Van den Bossche, J., Peters, J., Verwaeren, J., Botteldooren, D., Theunis, J., De Baets, B., 2015. Mobile monitoring for mapping spatial variation in urban air quality: development and validation of a methodology based on an extensive dataset. Atmos. Environ. 105, 148–161. https://doi.org/10.1016/j.atmosenv.2015.01.017.

Van Poppel, M., Peters, J., Bleux, N., 2013. Methodology for setup and data processing of mobile air quality measurements to assess the spatial variability of concentrations in urban environments. Environ. Pollut. 183, 224–233. https://doi.org/10.1016/j.envpol.2013.02.020.

Wen, Y., Wang, H., Larson, T., Kelp, M., Zhang, S., Wu, Y., Marshall, J.D., 2019. On-highway vehicle emission factors, and spatial patterns, based on mobile monitoring and absolute principal component score. Sci. Total Environ. 676, 242–251. https://doi.org/10.1016/j.scitotenv.2019.04.185.

Williams, R.D., Knibbs, L.D., 2016. Daily personal exposure to black carbon: a pilot study. Atmos. Environ. 132, 296–299. https://doi.org/10.1016/j.atmosenv.2016.03.023.